Acta Cryst. (1952). **5**, 606

On the Crystal Structures, Residual Entropy and Dielectric Anomaly of Methanol

By Kenneth J. Tauer and William N. Lipscomb

School of Chemistry, University of Minnesota, Minneapolis 14, *Minnesota, U.S.A.*

(*Received* 17 *November* 1951 *and in revised form* 27 *February* 1952)

The orthorhombic form of methanol has the space group D_{2h}^{17}–*Cmcm*. There are four molecules in a unit cell of dimensions $a=6{\cdot}43$, $b=7{\cdot}24$ and $c=4{\cdot}67$ Å. Infinite zigzag chains of hydrogen bonds exist parallel to the (100) face. The C–O distance is 1·42 Å, and the O · · · O hydrogen-bond distance is 2·66 Å, indicating strong hydrogen bonds. Surrounding a particular methyl, there are two methyls at 3·88 Å, four methyls at 4·01 Å, two oxygens at 3·86 Å and four oxygens at 4·09 Å.

The diffraction effects obtained from single crystals cooled through the λ point indicate that the transition is a simple displacive transformation involving a puckering of the infinite hydrogen-bonded chains, preserving the infinite chains of hydrogen bonds. The essential aspects of this transformation may be described by a monoclinic unit, containing two molecules, with $a=4{\cdot}53$, $b=4{\cdot}69$, $c=4{\cdot}91$ Å and $\beta=90°$ in the space group C_{2h}^{2}–$P2_1/m$, although the presence of some weak reflections suggests a superlattice. It is concluded that the residual entropy is zero, and that the dielectric anomaly is associated with the puckering of the chains discussed above.

Introduction

The X-ray diffraction studies of methanol were undertaken to elucidate the nature of the transition at the λ point and to determine whether the structure stable at the low temperatures would allow for residual entropy. Parks (1925) observed the λ point at 161·1° K.; Kelley (1929) fixed the temperature of maximum heat capacity at 157·4° K. and suggested that the transition was similar to that of ammonium chloride. With these third-law entropy data available, statistical entropy calculations were made to establish the value of the residual entropy, together with a reasonable value of the potential hindering rotation of the methyl group. These attempts have recently been reviewed by Halford (1950) who favors a residual entropy of 0·4–0·5 e.u., but remarks that the data are not sufficiently accurate to exclude zero residual entropy. Weltner & Pitzer (1951) found that by taking account of the gas-phase polymerization, attributed to tetramers, it was possible without the assumption of residual entropy to bring the various thermodynamic quantities into agreement with calculated values using a reasonable value of 932 cal./mole for the hindering potential.

Other studies bearing on the problem undertaken here are X-ray diffraction studies of liquid methanol at 198° K. (Zachariasen, 1935; Harvey, 1938). Harvey's study led to a C–O distance of 1·5 Å and an O · · · O hydrogen-bond distance of 2·7 Å. A study of the strength of the hydrogen bonds in methanol through the shift of the O–H vibration frequency (Badger, 1940) led to an estimate of 7500 cal./mole. A C–O distance of $1{\cdot}43\pm0{\cdot}01$ Å is reported from the spectroscopic study by Koehler & Dennison (1940). An electron-diffraction study (Kimura, 1950) gave a C–O distance of $1{\cdot}48\pm0{\cdot}04$ Å, which is significantly greater than the C–O distance of 1·42 Å found in the ethers. A more precise determination of the C–O distance by the electron-diffraction method has been made by Lu & Schomaker (cited by Allen & Sutton, 1950), who gave $1{\cdot}44\pm0{\cdot}01$ Å. The value which we obtain here ($1{\cdot}42\pm0{\cdot}03$ Å) is less precise than the value given by Lu & Schomaker, and must be regarded as in good agreement with their value.

Staveley & Gupta (1949), who studied the transition both in methanol and in methyl deuteroxide, suggested that the transition was similar to that of resorcinol. By extrapolating the specific-heat curves to the λ point, they calculated the heat of transition to be 170 ± 2 cal./mole.

The variation of the dielectric constant of methanol at the transition and at the melting point (Smyth & Hitchcock, 1934; Smyth & McNeight, 1936) led to the conclusion that in the form stable above the transition the entire molecule is rotating, while below the transition the low value may be accounted for by molecular polarization alone.

The present investigation supplements these previous studies, and in the case of the large increase of dielectric constant at the λ point, suggests an explanation not involving rotation of the entire molecule.

Experimental

Commercial methanol was purified by triple fractional crystallization and was then distilled into thin-walled pyrex capillary tubes of approximately 0·5 mm. diameter. The methanol was then frozen with liquid nitrogen and the tubes were sealed off under vacuum. Results obtained with capillaries sealed off in contact with air were not noticeably different. The Buerger

precession and Weissenberg photographs were taken with Mo $K\alpha$ radiation, using techniques described elsewhere (Abrahams, Collin, Lipscomb & Reed, 1950; Reed & Lipscomb, to be published). The multiple-film method was employed, the films being interleaved with 0·001 in. brass foil. The higher-temperature photographs were taken at approximately −110° C. and the low-temperature photographs at approximately −160° C. The observed F's were derived from visually estimated intensities, using standard scales. The Lorentz and polarization factors for the precession photographs were obtained from Evans, Tilden & Adams (1949). For photographs for which the precession angle was increased to 28° by virtue of redesign of the cooling system, the Lorentz factor, as corrected by Waser (1951), was used. Both modifications showed negative tests for pyroelectricity.

Structure determination of the −110° C. modification

Methanol, molecular weight 32·042, melts at 175·37° K. and undergoes a λ-point transition at 157·8° K. (Staveley & Gupta, 1949). Since the high-temperature form does not supercool appreciably, considerable difficulty was encountered in keeping the temperature within this range. Precession photographs obtained were zero- and first-level about [100], [010], and [1$\bar{1}$0]; Weissenberg photographs obtained were zero- and first-level about [001] and [1$\bar{1}$0]. The diffraction maxima showed Laue symmetry D_{2h}–mmm with the systematic extinctions of hkl with $h+k$ odd, $h0l$ with h odd and l odd independently and therefore $00l$ with l odd. The possible space groups are D_{2h}^{17}–$Cmcm$, C_{2v}^{16}–$C2cm$, C_{2v}^{12}–$Cmc2_1$. The orthorhombic cell has the dimensions

$$a=6\cdot43\pm0\cdot02,\ b=7\cdot24\pm0\cdot02,\ c=4\cdot67\pm0\cdot02\ \text{Å},$$

and a volume of 218 Å^3. Assumption of four molecules per unit cell gives a calculated density of 0·972 g.cm.$^{-3}$ as compared with an observed density* of approximately 0·98 g.cm.$^{-3}$.

With the assumption that carbon and oxygen were distinguishable, and with qualitative considerations of the intensities, it was easy to eliminate special positions in these space groups and to reduce the parameters to a consideration of the following fourfold positions:

C_{2v}^{12}: $0, y, z;\ 0, \bar{y}, \frac{1}{2}+z;\ \frac{1}{2}, \frac{1}{2}+y, z;\ \frac{1}{2}, \frac{1}{2}-y, \frac{1}{2}+z;$
C_{2v}^{16}: $x, y, \frac{1}{4};\ x, \bar{y}, \frac{3}{4};\ \frac{1}{2}+x, \frac{1}{2}+y, \frac{1}{4};\ \frac{1}{2}+x, \frac{1}{2}-y, \frac{3}{4};$
D_{2h}^{17}: $0, y, \frac{1}{4};\ 0, \bar{y}, \frac{3}{4};\ \frac{1}{2}, \frac{1}{2}+y, \frac{1}{4};\ \frac{1}{2}, \frac{1}{2}-y, \frac{3}{4}$.

Approximate atomic positions were found from the Patterson section $P(x, y, \frac{1}{2})$, which gave peaks at $x = 0$, $y = 0{\cdot}62$ Å and $x = 0$, $y = 1{\cdot}27$ Å, and the Patterson projection $P(y)$, which gave a peak at 1·23 Å probably displaced somewhat by the central peak. Because we expected displacements from the centrosymmetric space group D_{2h}^{17} owing to the tendency of oxygen to form tetrahedral bonds, the refinement of the projection $\varrho(x, y)$ in C_{2v}^{16} was attempted. However, both with and without the inclusion of hydrogen contributions, $\varrho(x, y)$ refined to the centrosymmetric projection which can be derived either from C_{2v}^{12} or D_{2h}^{17}. Displacements of the type demanded by C_{2v}^{12} were then considered in the calculation of $\varrho(y, z)$, but this projection also refined to the centrosymmetric D_{2h}^{17}, which we therefore regard as the correct space group. The calculated values of the reflections (220), (440) and (022) were so small that their signs were determined by the criterion of minimizing the background of these

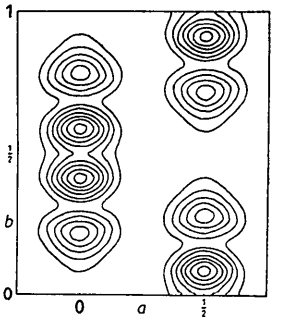

Fig. 1. The electron-density projection $\varrho(x, y)$. Contour levels are at 1, 2, 3, ...7 e.Å^{-2}.

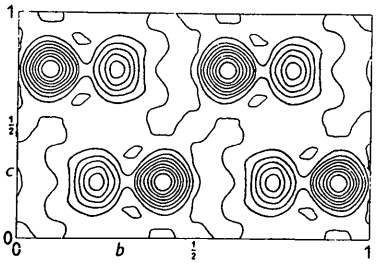

Fig. 2. The electron-density projection $\varrho(y, z)$. Contour levels are at ½, 1, 2, 3, ...8 e.Å^{-2}.

electron-density maps, shown in Figs. 1 and 2. Corrections for non-convergence of series were made by comparison with electron-density maps made from calculated data, and, except for y_C of $\varrho(y, z)$ for which the correction was −0·005, these corrections were 0·002 or less. The final values of the parameters are $y_C = 0{\cdot}215$, $y_O = 0{\cdot}410$ from $\varrho(y, z)$ (precession data) and $y_C = 0{\cdot}214$, $y_O = 0{\cdot}411$ from $\varrho(x, y)$ (Weissenberg data). In calculating average parameters we have regarded the Weissenberg data as somewhat more nearly convergent, and have weighted the values according to the errors suggested by the back-shift corrections. Thus our final average parameters are $y_C = 0{\cdot}214\pm0{\cdot}003$ and $y_O = 0{\cdot}410_5\pm0{\cdot}002$.

The ellipticity of the contours of $\varrho(x, y)$, produced

* This value is the result of an approximate calculation from the density of liquid methanol and the volume contraction observed upon solidification.

Table 1. *Comparison of structure factors for the* −110° C. *modification of methanol*

hkl	F_o	F_c	*hkl*	F_o	F_c	*hkl*	F_o	F_c
200	35	34	402	7	4	422	< 4	1
400	8	6	021	13	13	423	< 4	3
600	< 4	7	022	3	1	424	< 5	1
020	6	4	023	7	7	621	< 4	2
040	3	3	024	< 4	2	131	7	7
060	8	7	025	3	3	132	< 3	3
080	< 4	1	041	16	13	133	4	3
002	25	27	042	3	0	134	< 4	3
004	9	11	043	7	9	331	< 2	4
110	18	15	061	4	5	332	< 2	3
130	9	3	062	7	6	333	< 2	3
150	12	12	063	3	4	531	< 4	2
170	< 4	0	081	< 5	0	532	< 4	2
220	4	1	111	27	27	241	10	12
240	< 3	3	112	11	12	242	< 4	2
260	6	5	113	8	10	243	4	6
310	6	6	114	4	4	244	< 4	0
330	3	1	115	< 5	5	441	3	2
350	6	6	311	10	9	442	< 2	1
370	< 4	1	312	4	5	443	< 6	5
420	< 3	1	313	4	5	641	< 5	5
440	2	0	314	< 4	2	151	6	5
460	< 4	4	511	4	0	351	4	2
510	< 3	4	711	< 4	5	352	4	5
530	< 3	2	221	8	8	353	< 4	3
550	< 4	6	222	< 2	1	551	< 4	3
620	< 4	2	223	5	4	261	4	4
640	< 4	0	224	2	1	461	< 2	4
202	16	17	225	< 5	2	161	4	3
204	6	8	421	< 4	4			

by the exaggerated decline of reflections with increasing h index, indicated an anisotropic temperature factor with the direction of maximum vibration perpendicular to (100), and thus normal to the plane of the chains. The best fit of observed data with the temperature factor $\exp\{-[B_1+B_2\cos^2(h.a)]\sin^2\theta/\lambda^2\}$ showed that $B_1 = B_2 = 4$Å^2.

Table 1 lists observed and calculated structure factors. The figure of merit $\Sigma||F_c|-|F_o||\div\Sigma|F_o|$ is 0·17, for which only observed reflections have been included.

A diagram of the structure is shown in Fig. 3. The

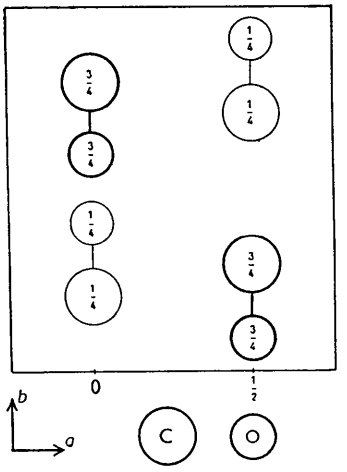

Fig. 3. Structure of the high-temperature form projected along the c axis of the orthorhombic cell.

interatomic and intramolecular distances and angles are as follows:

C–O bonded	1·42±0·03 Å
O · · · O hydrogen bond	2·66±0·03 Å
C–O · · · O angle	118·9±2°
$CH_3 \cdots CH_3$	3·88 and 4·01 Å
$CH_3 \cdots O$	3·86 and 4·09 Å

The C–O distance corresponds with the similar bond in the ethers, and is insignificantly shorter than the electron-diffraction result of 1·44±0·01 Å for methanol (Lu & Schomaker, 1950). The O · · · O hydrogen-bond distance agrees well with a predicted distance assuming proportionality among the frequency shift of the O–H stretching frequency, the energy of the bond and the O · · · O distance of the bond. Badger (1940) was led to a value of 7500 cal./mole for the hydrogen-bond energy from the frequency shift. Assuming an inverse correlation of bond energy and interatomic distance for O · · · O hydrogen bonds, a distance less by 0·02 Å than the formic acid value of 2·73 Å (7·1 kcal./mole) would be predicted (Pauling, 1940; Karle & Brockway, 1944).

The C–O · · · O bond angle of 118·9° is considerably different from that anticipated. Assuming that the unshared electron pair would retain more of the more firmly bound s orbital character, there would not be complete hybridization and the expected angle would be something less than the tetrahedral angle of 109·5° (Koehler & Dennison (1940) give 104·5°). However, if we assume that the hydrogen lies along the O · · · O

distance, packing effects have considerable influence in modifying bond angles in crystals. The closest methyl–methyl approach of 3·88 Å is less than would be expected for a methyl group of radius 2·0 Å but it agrees with the approaches in other reasonably well packed structures such as metaldehyde, 3·90 Å, (Pauling & Carpenter, 1936), threonine, 3·79 Å, (Shoemaker, Donohue, Schomaker & Corey, 1950) and alanine, 3·64 Å, (Levy & Corey, 1941). A methyl group is thus surrounded by two methyls at 3·88 Å, four methyls at 4·01 Å, two oxygens at 3·86 Å and four oxygens at 4·09 Å. Methanol is only a reasonably well packed structure, particularly in view of the large thermal motion of approximately 0·32 Å r.m.s. amplitude of vibration perpendicular to the (100) face ($B = 8\pi^2\mu^2$). The increase in van der Waals and polarization energies through better packing probably overcomes the decrease in hydrogen-bond energy caused by the deformation of the near-tetrahedral configuration, and hence renders the structure more stable. The same type of behavior is exhibited by β-resorcinol (Robertson & Ubbelohde, 1938).

Study of the −160° C. modification

About 12 different crystals of the β (higher-temperature) phase were cooled through the λ point. The resulting crystals of the α (low-temperature) phase were obviously not single, and while our interpretation of the resulting diffraction effects indicates the main features of chemical interest, a complete and unique description of the α phase cannot be claimed.

A few of the diffraction photographs of both phases are shown in Figs. 4 and 5. The reciprocal-lattice plot derived from the zero-level Weissenberg photograph about this same axis is shown in Fig. 6. As indicated, the reflections of this photograph, and of photographs of the first and second levels about this axis, are streaked over a range of 15–20° depending on the intensity of the reflection, and increasing slightly with increasing values of $\sin\theta$. Since the precession photographs showed only sharp spots, we conclude that these streaks are short ones in reciprocal space lying in planes parallel to the $a\,b$ plane of the β phase.

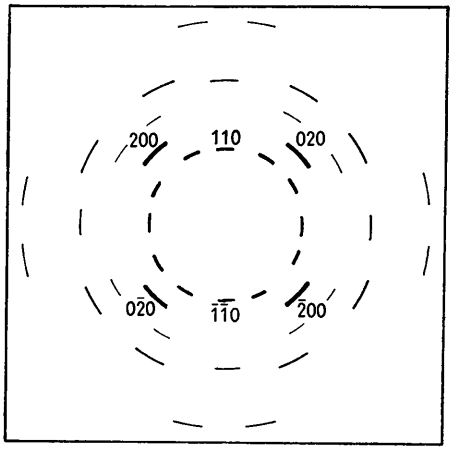

Fig. 6. Reciprocal-lattice plot of the $h0l$ data from the zero-level b-axis Weissenberg photograph. Indices correspond to the unit cell of the high-temperature phase. The transformation changes (110) into (100), (200) into (10$\bar{1}$), etc. The temperature of the crystals was −160° C.

Our major conclusions from these diffraction photographs, and the supporting evidence are as follows:

(1) The same system of hydrogen bonds is present in both phases. These hydrogen bonds are along the $c = 4{\cdot}67$ Å axis of the β phase, which becomes the $b = 4{\cdot}69$ Å axis of the α phase in the transformation. Within experimental error these two dimensions are equal. Further support is given below in § 2.

(2) The transformation is of the displacive type (Buerger, 1945), involving only a puckering of the infinite chains in order to achieve more compact packing; the displacements are confined to planes normal to the direction of the infinite chains of hydrogen bonds. Support for this conclusion comes from the normal decline of odd orders of $0k0$ reflections of the α phase, compared with the same normal decline of the odd orders of the $00l$ reflections of the β phase. Thus the projection of electron density on the axis lying along the chain direction is identical in both phases. Even stronger support is provided by the essentially identical relative intensities of the zero- and second-level Weissenberg photographs about the b axis of the α phase. Both conclusions (1) and (2) are supported by the low heat of transition of 170 cal./mole (Staveley & Gupta, 1949), which makes likely only minor structural changes in the transition and is consistent with the preservation of the system of relatively strong hydrogen bonds.

(3) The transition probably involves only such displacements of atoms in the planar infinite chains in the β phase to give puckered infinite chains in the α phase. This conclusion is indicated by the shortening of the repeat distance along which the axis of the molecules lie from 7·24 Å in the β phase to 6·67 Å in the α phase. This puckering seems very reasonable from a structural point of view because of the tendency which oxygen has to form tetrahedral, instead of planar, bonds. The unusually high amplitude of thermal motion along the a axis of the β phase suggests a rapid interchange of the two puckered, collapsed forms of these infinite chains, and the transition might well be expected to involve some modification of this particularly large amplitude.

(4) The α phase probably consists of small crystallites of relatively low symmetry, mutually oriented approximately 90° about the c axis of the β phase. This conclusion is strongly suggested by the appearance of two distinct reciprocal-net planes in Fig. 5(*b*), and by the essentially identical low-temperature photograph (Fig. 5(*a*)) given by both the $h0l$ and the $0kl$ nets of the β phase (Fig. 4(*a*) and (*b*)). Thus it is quite clear that our low-temperature phase was not a single crystal.

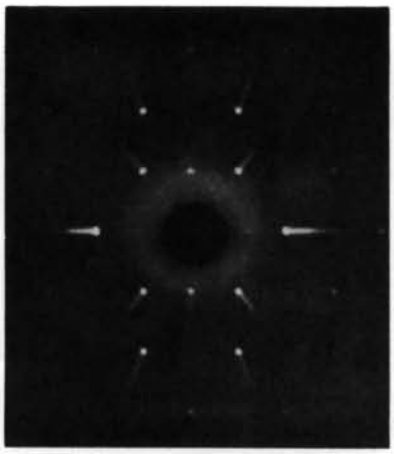

Fig. 4(*a*). Precession photograph of the 0*kl* net at −110° C.

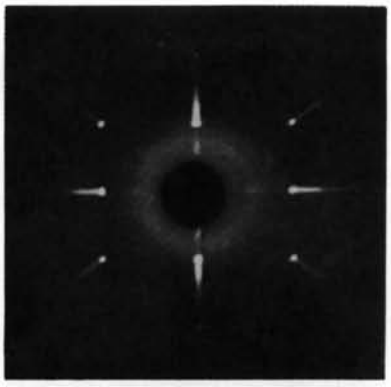

Fig. 4(*b*). Precession photograph of the *h*0*l* net at −110° C.

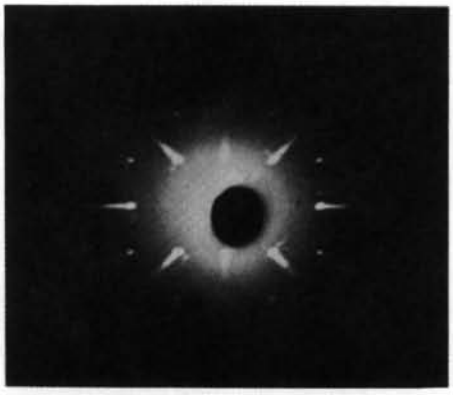

Fig. 4(*c*). Precession photograph of the *hhl* net at −110° C.

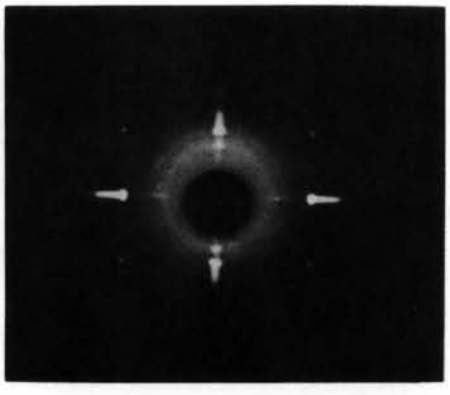

Fig. 5(*a*). Precession photograph at −160° C. corresponding to both the *h*0*l* and 0*kl* nets at −110° C. These are the *hkh* nets for the centrosymmetric monoclinic cell.

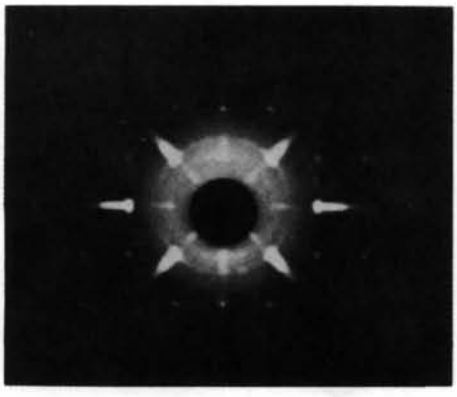

Fig. 5(*b*). Precession photograph at −160° C. corresponding to the *hhl* net at −110° C. This photograph includes the *hk*0 and 0*kl* nets of the centrosymmetric monoclinic cell.

[*To face p.* 609

(5) The crystallites of the α phase are misaligned over a range of approximately 8–10° in the plane normal to the direction of the hydrogen bonds. This is the type of disorder suggested to us by the streaking of reflections on the Weissenberg photographs, and is consistent with our interpretation of the transformation as a simple displacive one.

(6) A possible unit cell, which accounts for the positions and intensities of all but a very few faint reflections, is monoclinic with two molecules in a unit with dimensions $a = 4{\cdot}53 \pm 0{\cdot}03$, $b = 4{\cdot}69 \pm 0{\cdot}02$, $c = 4{\cdot}91 \pm 0{\cdot}03$ Å, and $\beta = 90 \pm 3°$. With this unit the *hkh* photograph (Fig. 5(*a*)) has both *hkh* and *hkh̄* nets, while the *hk*0 or 0*kl* photographs (Fig. 5(*b*)) each include both *hk*0 (outer set) and 0*kl* (inner set) reflections. The extinction of 0*k*0 for *k* odd places this modification in either C_{2h}^2–$P2_1/m$ or C_2^2–$P2_1$. Assuming carbon and oxygen non-equivalent, the only applicable positions of C_{2h}^2 are the twofold special positions 2(*e*) to which C_2^2 reduces in view of the normal decline of 0*k*0; thus the consideration of parameters is reduced to x, $\frac{1}{4}$, z and $\bar{x}$, $\frac{3}{4}$, $\bar{z}$.

As a result of the mutual orientation of the crystals, it is impossible to determine intensities for individual reflections except for the *hk*0 and 0*kl* nets which are sufficiently separated. Trial-and-error procedures were now resorted to in order to determine the values of the parameters, and the best fit of calculated and observed data with a temperature factor of $B = 1{\cdot}2$ Å^2 was obtained from the parameters, $x_C = 0{\cdot}25$, $z_C = 0{\cdot}16$, $x_O = 0{\cdot}37$ and $z_O = 0{\cdot}43$, all $\pm 0{\cdot}01$ or slightly greater. Table 2 shows the agreement between the observed and calculated structure factors. Except for *hk*0 and 0*kl* reflections, the F_c are the result of r.m.s. average of the calculated structure factors for the mutually oriented fragments. The contribution of the hydrogen atoms was included by assumption of a tetrahedral methyl group (C–H = 1·09 Å) rotating about the C–O axis. The observed F's were derived from visual estimates using standard scales and the usual Lorentz and polarization factors, except for the Weissenberg photographs for which the intensities were obtained by means of a Leeds and Northrup Knorr-Albert densitometer.

Comparatively faint superlattice reflections appear on the *hkh* photographs and on the Weissenberg photographs. A possible way in which these may be accounted for is the doubling illustrated by the molecular configuration shown in broken lines in Fig. 7. The structure factors for these two possible structures appear in Table 2. The agreement for the undoubled cell is somewhat decreased by this distortion, and consequently some further modifications of atomic positions are desirable, but, in view of the many possible ways of distorting the structure and of the quality of the data, we have not proceeded further.

The interatomic and intramolecular distances and angles of the undoubled cell (solid lines) in Fig. 7 are as follows:

C–O bond distance	1·44 Å
O · · · O hydrogen bond	2·68 Å
C–O · · · O angle	108°
$CH_3 \cdots CH_3$	3·64 Å
$CH_3 \cdots O$	4·1 and 4·2 Å
O · · · O	4·0 Å

The configuration shown in broken lines in Fig. 7 required to satisfy the super-lattice reflections increases the closest methyl–methyl approach to 3·74 Å, thus suggesting a possible reason for the doubling of the cell.

Table 2. *Structure factors of the low-temperature phase*†

$hkl^{\pm}$	F_o	$F_c^{\pm}$	F_c^*	$hkl^{\pm}$	F_o	$F_c^{\pm}$	F_c^*
100	9	9	5	013	< 4	6	8
200	5	6	5	021	< 4	6	5
300	4	5	5	022	4	3	3
110	24	17	17	023	< 4	5	5
210	6	9	9	031	7	6	7
310	< 4	3	3	032	< 4	1	2
120	6	6	3	101(10$\bar{1}$)	18	18	17
220	4	4	4	102(20$\bar{1}$)	8	8	6
320	< 4	4	4	103(30$\bar{1}$)	6	7	5
130	7	8	8	201(10$\bar{2}$)	9	5	6
230	3	5	6	301(10$\bar{3}$)	6	6	9
001	< 4	4	5	121(12$\bar{1}$)	8	11	10
002	5	5	5	141(14$\bar{1}$)	3	6	5
003	4	6	6	212(21$\bar{2}$)	7	8	8
011	18	12	13	232(23$\bar{2}$)	4	5	5
012	< 4	2	4				

† The $hkl^{\pm}$ and $F_c^{\pm}$ refer to the structure shown by solid lines in Fig. 7, while the hkl^* and F_c^* refer to the broken lines. Those reflections which require a larger unit cell, and which have either F_o or F_c^* greater than 4·0, are (201)*, 8, 5; (20$\bar{1}$)*, 8, 3; (221)*, 6, 3; (113)* and (311)*, < 4, 6; (11$\bar{5}$)* and (21$\bar{3}$)*, < 4, 4. In this listing F_c^* is the latter value. In all cases where more than one reflection occurs in the same region of the film (owing to the 90° mutual orientation of crystallites), the mean value, $F_c = \sqrt{\sum_i F_{c\,i}^2}$, is tabulated.

It is felt that the data obtained are not sufficient to determine unambiguously the exact configuration stable below the transition. However, we feel that

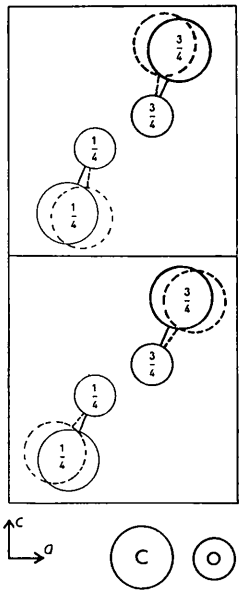

Fig. 7. Structure of the low-temperature form projected along the b axis of the monoclinic cell. The configuration shown by broken lines is a possible distortion which accounts for the superlattice spots appearing on Fig. 5(a) and Fig. 6.

these data are sufficient to establish the essentials of the nature of the transition and, to a reasonably good approximation, the molecular configuration stable below the transition.

The residual entropy

Considerable effort has been directed toward the resolution of a seeming discrepancy between the statistical entropy and the third-law entropy of methanol. Halford (1950) has reviewed these attempts and concludes that while the available data are not sufficiently accurate to exclude zero residual entropy, they suggest a residual entropy of 0·4 to 0·5 e.u. Since the thermochemical data are sufficiently reliable, and the molecular geometry and vibrational assignments satisfactorily established, the least reliable data are the entropy corrections due to gas imperfections and the entropy of internal rotation. Weltner & Pitzer (1951) have determined an equation of state from heat-capacity measurements at different pressures and found that previous calculations were principally in error because of a wrong assumption of the equation of state. These measurements indicated an unusually large entropy correction for gas imperfections, particularly due to an indicated gas-phase polymerization, presumably into tetramers. The comparatively high energy hydrogen bonds formed by methanol indicated by the O–H frequency shift (Badger, 1940) and in the present investigation by the short O · · · O distance also make the gas-phase polymerization very reasonable. By virtue of the large entropy of gas imperfection, Weltner & Pitzer have brought the various thermodynamic quantities into agreement without the assumption of significant residual entropy. We feel that the present investigation has established beyond reasonable doubt that the low-temperature form of methanol retains the infinite chains of hydrogen bonds shown to exist in the form stable above the transition, and thus, from a structural standpoint, it cannot retain appreciable residual entropy.

The dielectric anomaly

Smyth & Hitchcock (1934) and Smyth & McNeight (1935) have measured the dielectric constant of methanol as a function of temperature and found the expected decrease at the freezing point; however, the value between the transition and the melting point is considerably higher than that expected from polarization of individual molecules alone. Below the transition the dielectric constant dropped to a value so low as evidently to arise almost wholly from such molecular polarization. Their interpretation of these data is that below the melting point the dipoles are still free of orientation in the lattice and that this freedom is attenuated as the temperature decreases and disappears completely at the λ point. Since methanol is the only alcohol exhibiting this behavior, it is concluded that the freedom of dipole orientation must be due to a rotation of the entire molecule rather than of the hydroxyl group within the molecule. The results of our investigation show that the large dielectric constant between the transition and the melting point cannot be due to molecular rotation or to rotation of the hydroxyl groups within the molecule, but very likely that the freedom of dipole orientation observed is that due to the interchange of the two collapsed forms of which the high temperature form is the statistical average. The observed large thermal motion of the molecules perpendicular to the planes containing the infinite chains of hydrogen bonds adequately substantiates this interpretation. Similarly, the rapid decrease of the dielectric constant with frequency above the transition, observed by Smyth & Hitchcock, is consistent with this interpretation. It would obviously be of interest to measure the dielectric constant of single crystals in various directions.

An alternative explanation is that cooperative polarization of the hydrogen bonds occurs, but our cell dimensions and structures indicate that this polarization would occur both above and below the transition, and therefore this effect can hardly be significantly greater above the transition.

We wish to acknowledge with thanks financial aid from the Office of Naval Research, and also to thank Dr W. J. Dulmage, Mr R. M. Curtis, Mr L. R. Lavine, Mr C. E. Nordman, and Miss Lies Nijssen for assistance

in the experimental work and in the preparation of drawings.

Bibliography

ABRAHAMS, S. C., COLLIN, R. L., LIPSCOMB, W. N. & REED, T. B. (1950). *Rev. Sci. Instrum.* **21**, 396.
ALLEN, P. W. & SUTTON, L. E. (1950). *Acta Cryst.* **3**, 46.
BADGER, R. M. (1940). *J. Chem. Phys.* **8**, 288.
BUERGER, M. J. (1945). *Amer. Min.* **30**, 469.
EVANS, H. T., TILDEN, S. G. & ADAMS, D. P. (1949). *Rev. Sci. Instrum.* **20**, 155.
HALFORD, J. O. (1950). *J. Chem. Phys.* **18**, 361.
HARVEY, G. G. (1938). *J. Chem. Phys.* **6**, 111.
KARLE, J. & BROCKWAY, L. O. (1944). *J. Amer. Chem. Soc.* **66**, 574.
KELLEY, K. K. (1929). *J. Amer. Chem. Soc.* **51**, 180.
KIMURA, M. (1950). *J. Chem. Soc. Japan.* (Pure Chem.) **71**, 18.
KOEHLER, J. S. & DENNISON, D. M. (1940). *Phys. Rev.* **57**, 1006.
LEVY, H. A. & COREY, R. B. (1941). *J. Amer. Chem. Soc.* **63**, 2095.
PARKS, G. S. (1925). *J. Amer. Chem. Soc.* **47**, 338.
PAULING, L. & CARPENTER, D. C. (1936). *J. Amer. Chem. Soc.* **58**, 1274.
PAULING, L. (1940). *The Nature of the Chemical Bond*, 2nd ed. Ithaca: Cornell University Press.
ROBERTSON, J. M. & UBBELOHDE, A. R. (1938*a*). *Proc. Roy. Soc.* A, **167**, 122.
ROBERTSON, J. M. & UBBELOHDE, A. R. (1938*b*). *Proc. Roy. Soc.* A, **167**, 136.
SHOEMAKER, D. P., DONOHUE, J., SCHOMAKER, V. & COREY, R. B. (1950). *J. Amer. Chem. Soc.* **72**, 2328.
SMYTH, C. P. & HITCHCOCK, C. S. (1934). *J. Amer. Chem. Soc.* **56**, 1084.
SMYTH, C. P. & MCNEIGHT, S. A. (1936). *J. Amer. Chem. Soc.* **58**, 1597.
STAVELEY, L. A. K. & GUPTA, A. K. (1949). *Trans. Faraday Soc.* **45**, 50.
WASER, J. (1951). *Rev. Sci. Instrum.* **22**, 567.
WELTNER, W. & PITZER, K. S. (1951). *J. Amer. Chem. Soc.* **73**, 2606.
ZACHARIASEN, W. H. (1935). *J. Chem. Phys.* **3**, 158.

Acta Cryst. (1952). **5**, 612

The Interference Theory of Ideal Paracrystals

BY R. HOSEMANN

AEG-Röntgenlaboratorium, Sickingenstr. 71, *Berlin NW* 87, *and Kaiser-Wilhelm-Institut für physikalische Chemie, Berlin-Dahlem, Germany*

AND S. N. BAGCHI

University College of Science, Calcutta, India

(*Received* 10 *September* 1951 *and in revised form* 28 *January* 1952)

The concept of a distorted lattice, 'ideal paracrystal', and its diffraction theory lead to a generalization of other well known interference theories and, in particular, under certain special conditions, degenerate to the theory of crystals by von Laue and Bragg, to that of liquids by Debye & Menke and Zernicke & Prins, and to that of amorphous matter by Guinier–Warren–Hosemann.

No single comprehensive theory of X-ray diffraction by matter of all kinds exists at present. There are three principal theories, namely the theory of X-ray diffraction by crystals by Laue (1913) and Bragg (Bragg & Bragg, 1913), that of liquids by Zernicke & Prins (1927) and Debye & Menke (1931), and that of 'amorphous' matter by Guinier (1939*a*, *b*) and Hosemann (1939), but the exact domain of validity of each of these is not clearly defined. Often for a single substance, e.g. a high polymer, the simultaneous existence of 'crystalline', 'liquid' and 'amorphous' features of the material is suggested. Various authors (Kratky, 1933, 1946; Hermans, 1944; Hermans & Weidinger, 1948; Warren, 1941; Bear & Bolduan, 1951; Fournet & Guinier, 1949) have tried to explain the X-ray diagrams by using additional hypotheses, but unfortunately no single theory explains satisfactorily all the characteristic features of the interference phenomena.

The concept of the 'ideal paracrystal' and the theory of its X-ray diffraction as given by Hosemann (1950*a*, *b*) is a step to fill up the gap in this direction. This theory uses the convolution or *Faltung* of Fourier transformation, the importance of which in the interference theories was first pointed out by Ewald (1940) and Hermans (1944).

Let there be N particles, each containing M electrons. According to the crystal theory, the scattered intensity at any angle is proportional to N^2M^2, whereas in the interference theory of liquids it is proportional to NM^2. 'Particle' in the first case stands for the total number of atoms in a lattice cell, and in